Journal of Organometallic Chemistry, 475 (1994) 267–276

Heterobimetallic heptamethylindenyl complexes of Cr^0 and Rh^I: *trans*-[$Cr(CO)_3$-indenyl*-RhL_2] (L_2 = COD, L = CO)

Chiara Bonifaci, Alberto Ceccon, Alessandro Gambaro, Paolo Ganis *, Laura Mantovani and Saverio Santi

Dipartimento di Chimica Fisica, Università di Padova, Via Loredan 2, I-35131 Padova (Italy)

Alfonso Venzo

CNR, Centro di Studio sugli Stati Molecolari, Radicalici ed Eccitati, Via Loredan 2, I-35131 Padova (Italy)

(Received January 17, 1994)

Abstract

Indenyl-RhL_2 species are efficient catalysts in the cyclotrimerization reaction of alkynes to give substituted arenes. The syntheses and X-ray structures of the two bimetallic complexes, *trans*-$Cr(CO)_3$-heptamethylindenyl-Rh(COD) and *trans*-$Cr(CO)_3$-heptamethylindenyl-$Rh(CO)_2$, are reported. The contemporary coordination of the benzene ring with $Cr(CO)_3$ and permethylation of the indenyl ligand enhance substantially the reaction rate of the trimerization and the stability of the catalyst. Best results were obtained when the bidentate cycloocta-1,5-diene was used as an ancillary ligand.

Key words: Rhodium; Chromium; Indenyl; Catalysis; Heterobimetallics

1. Introduction

The high current interest in indenyl-ML_n (M = Co, Rh, Ir, Re, Fe, Mn; L = CO, olefin, phosphine, phosphite) stems from the enhanced reactivity shown by these complexes both in S_N2 substitution reactions [1,2] and, as catalysts, in cyclotrimerization of alkynes to benzenes and in the cyclocotrimerization of alkynes and nitriles to pyridines [3], compared to that of their cyclopentadienyl analogues. This behaviour has been attributed to a greater flexibility of the indenyl *vs.* cyclopentadienyl ligand to coordinate the five membered ring with different bonding modes. The formation of species in which the metal bonds to the five membered ring in an η^3 or η^1 fashion has been recently demonstrated in addition or substitution reactions of Fe [4], Re [5], and Ir [6,7] indenyl complexes.

In recent years we have been developing the chemistry of bimetallic indenyl complexes in which the benzene ring of the ligand is bonded to $Cr(CO)_3$, *viz.*, $Cr(CO)_3$-indenyl-ML_n [7–11]. In particular, we have demonstrated that the reactivity of monometallic indenyl-ML_n in ligand substitution reactions [9] as well as in catalyzed cyclotrimerization of alkynes [10] increases substantially if the benzene ring is coordinated to $Cr(CO)_3$ in a "transoid" arrangement. Therefore, these bimetallic complexes show a kinetic behaviour which we dubbed "extra-indenyl effect" [11].

The current use of η^5-pentamethylcyclopentadienyl (Cp^*) ligand as an alternative to Cp in $C_5R_5ML_n$ complexes is amply justified by the exceptional blend of stability and reactivity induced by the permethylation [12]. In an analogous manner some permethylated indenyl (Ind^*) complexes have recently been synthesized [13]; in particular, Marder, Basolo and coworkers investigated the structure and reactivity of Ind^*-$M(CO)_n$ complexes. It has been shown [14] that permethylation has no effect on the ground state structure of these molecules; in contrast, the steric demand on the substituted indenyl ligand does have a profound effect on the course of the carbonyl substitution by phosphorous ligands [15]. The permethylated complex is indeed

Correspondence to: Prof. Alberto Ceccon.
* On sabbatical leave from University of Napoli, Italy.

0022-328X/94/$7.00
SSDI 0022-328X(94)24528-Q

© 1994 – Elsevier Science S.A. All rights reserved

very crowded and the reduction in rate may once again be due both to the increased negative charge density on the ring and to an increased congestion around the metal atom.

Throughout our investigations on bimetallic indenyl complexes, we failed to obtain suitable crystals of *trans*-Cr(CO)$_3$-indenyl-Rh(CO)$_2$ complex, which was not very stable in solution. In view of the greater stability and crystallizability of the permethylated series, we have investigated the effect of permethylation in the bimetallic compounds. In particular, we have synthesized, and studied the reactivity of, the two bimetallic complexes *trans*-Cr(CO)$_3$-indenyl*-Rh(CO)$_2$ (**A**) and *trans*-Cr(CO)$_3$-indenyl*-Rh(COD) (**B**). A brief description of the crystal structure of the above mentioned species, together with that of the precursor (1-*exo*-CH$_3$)-[Cr(CO)$_3$-1,2,3,4,5,6,7-heptamethylindene (**C**) is also provided.

2. Results and discussion

The complexation with Cr(CO)$_3$ of 1,2,3,4,5,6,7-heptamethylindene (HInd*) produced, owing to the presence of the chiral carbon atom C$_1$, both the diastereisomers (1-*exo*-CH$_3$)- and (1-*endo*-CH$_3$)-Cr(CO)$_3$-HInd*, the 1-*exo*-CH$_3$ having the methyl group on the opposite side of the inorganic group with respect to the indene mean plane.

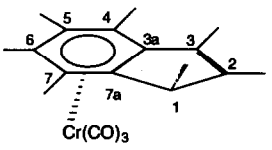

1-*exo*-CH$_3$

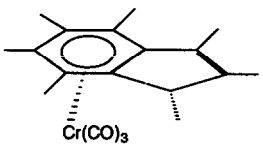

1-*endo*-CH$_3$

In the proton and carbon NMR spectra of the crude reaction mixture all the signals due to the two isomers appear well separated (see Experimental section), so that a product ratio 85:15 was measured by integration. The structure assignment to the two isomers was first accomplished by taking into account the proximity effect of the anisotropic Cr(CO)$_3$ unit on the 1-H and 1-CH$_3$ nuclei [16]. In fact, in the isomer obtained in the higher yield the downfield shift observed upon complexation for the signal of the 1-H proton is markedly higher than that for the 1-CH$_3$ protons, suggesting that the methine proton is closer to the inorganic moiety than the methyl protons. Exactly the reverse behaviour is shown by the second stereoisomer. Therefore, we confidently assigned the (1-*exo*-CH$_3$) arrangement to the former isomer and the (1-*endo*-CH$_3$) one to the latter isomer. The X-ray crystal structure determination (see below) confirmed this conclusion.

Abstraction of the proton from (1-*exo*-CH$_3$)-Cr(CO)$_3$- HInd* cannot be performed at -30°C by the use of the solvent/base system THF/KH, which was shown to be profitable for complete ionization of the non-methylated analogue [17]. Moreover, only partial ionization is obtained in the presence of the 18-crown-6 ether as an activating agent for the hydride. Lastly, the ionization cannot be performed above -30°C since the $\eta^6 \rightarrow \eta^5$ haptotropic movement of the inorganic unit occurs, as indicated by the IR spectra (ν(C≡O): η^6 anion, 1900, 1807, and 1788 cm^{-1}; η^5 anion, 1881 and 1769 cm^{-1}; counter-ion K$^+$/crown). The reduced acidity of the coordinated HInd* is very likely to be due to the electron releasing effect of the seven methyl groups, as indicated by the comparison of the carbonyl stretching frequencies with those observed for the non-methylated anion (ν(C≡O): η^6 anion, 1914, 1825, and 1802 cm^{-1}; η^5 anion, 1895 and 1791 cm^{-1}; counter-ion K$^+$/crown [17]). The complete ionization of (1-*exo*-CH$_3$)-Cr(CO)$_3$-HInd* was obtained in THF/hexane by using the TMEDA/LiBu base system. The nucleophilic addition to the benzene carbon atoms, which often competes with α-hydrogen abstraction, appears suppressed by the permethylation of the indene ligand. Also the (1-*endo*-CH$_3$)-Cr(CO)$_3$-HInd* isomer was found to be reactive towards the BuLi/TMEDA ionizing system.

The reaction of the [Cr(CO)$_3$-Ind*]$^-$ anion with [Rh(μ-Cl)(COD)]$_2$ is very fast even at low temperature and a moderate yield (*ca.* 30%) of Cr(CO)$_3$-Ind*-Rh(COD) was obtained which was quantitatively converted to the dicarbonyl derivative by bubbling CO through a CH$_2$Cl$_2$ solution. The permethylation makes the COD derivative much more stable in comparison with the non-methylated analogue, so that it can be purified by flash chromatography even at room temperature; also the obtaining of crystals suitable for diffractometry was easier. The monometallic Ind*-RhL$_2$ complexes were obtained similarly by starting from HInd*. The ^{1}H NMR spectrum of the permethylated mono and bimetallic rhodium complexes consists of a series of singlets due to the methyl groups in the (1,3), (4,7), and (5,6) positions, and of one doublet due to the 2-CH$_3$ protons which exhibit a coupling constant with the ^{103}Rh nucleus. The assignment of the proton resonances was performed by NOE measurements. In the ^{13}C NMR spectra a coupling between ^{103}Rh and all the quaternary carbons of the five membered ring is observed, together with a small coupling with the ^{13}C nucleus in the 2-CH$_3$ group. The electron releasing effect of the seven methyl groups induces a downfield

shift (*ca.* 2 ppm) both in the resonances of the carbon nuclei of $Cr(CO)_3$ and $Rh(CO)_2$ units.

The ^1H NMR spectra of the mono- and bimetallic Ind*-Rh(COD) species exhibit a temperature-dependent dynamic behaviour which is attributed to the kinetic of the rotation of the Rh(COD) group. As the temperature is lowered, the signal due to the olefinic protons of COD broadens, then it collapses (at T 170 K in the case of Ind*-Rh(COD), at T 217 K for the $Cr(CO)_3$ derivative), and finally it is manifested as two clearly distinct signals ($\Delta\nu$ 96 and 176 Hz, respectively). From these data, the activation free energy values $\Delta G^{\ddagger}$ 33 ± 1 and 42 ± 1 KJ mol^{-1} for the mono- and the bimetallic species, respectively, have been calculated [18].

2.1. X-ray measurements

Selected bond distances, bond and torsion angles for **A**, **B** and **C** are listed in Table 1 together with the parameters conventionally adopted to describe the modes of coordination of metals to arenic ligands, *i.e.* slip distortion (Δ), hinge angle (HA) and fold angle (FA) [14]. Specifically, these values indicate only slightly distorted η^6 and η^5 coordinations for Cr and Rh, respectively, in **A** and **B** and a true η^6 coordination for Cr in **C**. For the complex **B** the distortions are virtually equivalent to those of the corresponding unsubstituted complex, $Cr(CO)_3$(indenyl)Rh(COD) [8]. Therefore the permethylation of the indenyl ligand does not modify the overall molecular structure of these complexes, as recently reported for similar alkylated monometallic compounds [15]. This fact excludes the possibility that any different chemical behaviour in solution can be explained on the basis of crystal data.

Beyond these features, there are certain noteworthy geometrical parameters reported in Table 1 and illustrated in Figs. 1–3. The $Cr(CO)_3$ groups in **A** and **B** are disposed in the usual more stable "exo" conformation deviating from an idealized staggered orientation by 4–5° and 6–8°, respectively. In contrast, in the case of **C**, the $Cr(CO)_3$ group is in the quite uncommon "endo" conformation, and it is rotated by *ca.* 5° from a staggered orientation. A careful analysis of the mode of packing, considering that the exo and the endo structures are almost isosteric, seems to exclude any influence of crystal field on this feature. Moreover, the rotation of the $Cr(CO)_3$ group in the sense of a shorter distance of the endo CO group from the "cisoid" hydrogen atom bonded to C(1) (*ca.* 2.85 Å in this structure), suggests a probable attractive interaction between these molecular frames as found in many similar complexes [16] and this fact should justify the higher yield of the *exo* isomer with respect to that of the *endo* analogue.

TABLE 1. Selected geometrical parameters for *trans*-$Cr(CO)_3$-indenyl*-$Rh(CO)_2$ (**A**) *trans*-$Cr(CO)_3$-indenyl*-Rh(COD) (**B**), and (1-*exo*-CH_3)-[$Cr(CO)_3$-1,2,3,4,5,6,7-heptamethylindene] (**C**)

	A	B	C
Bond distances (Å)			
Cr–C(3a)	2.285(5)	2.321(7)	2.231(8)
Cr–C(4)	2.248(5)	2.239(6)	2.220(7)
Cr–C(5)	2.231(7)	2.221(6)	2.208(6)
Cr–C(6)	2.216(6)	2.202(6)	2.209(8)
Cr–C(7)	2.235(5)	2.230(7)	2.220(8)
Cr–C(7a)	2.257(6)	2.311(6)	2.232(8)
Rh–C(1)	2.205(4)	2.190(6)	
Rh–C(2)	2.232(8)	2.225(6)	
Rh–C(3)	2.234(6)	2.261(6)	
Rh–C(3a)	2.449(6)	2.390(5)	
Rh–C(7a)	2.405(6)	2.369(6)	
Rh–C(11)	1.851(6)	2.151(8)	
Rh–C(12)	1.860(6)	2.129(7)	
Rh–C(14)		2.131(7)	
Rh–C(15)		2.160(7)	
Bond angles (°)			
Cr–C(8)–O(8)	177.1(4)	178.0(5)	178.1(7)
Cr–C(9)–O(9)	178.3(6)	178.2(4)	177.1(8)
Cr–C(10)–O(10)	179.2(4)	180.1(4)	179.3(8)
Rh–C(11)–O(11)	172.5(5)		
Rh–C(12)–O(12)	177.3(8)		
Torsion angles (°) [a]			
C(7)–P–Cr–C(9)	−38	−33	−36
C(5)–P–Cr–C(8)	−38	−36	−35
C(3a)–P–Cr–C(10)	−36	−36	−35
Coordination parameters			
Δ_{Cr} (Å)	0.04	0.09	0.01
Δ_{Rh} (Å)	0.20	0.15	–
HA_{Cr} (°)	3	1	0
HA_{Rh} (°)	11	9	–
FA_{Cr} (°)	0	0	0
FA_{Rh} (°)	9	5	–

[a] P indicates the location of the benzene ring centre.

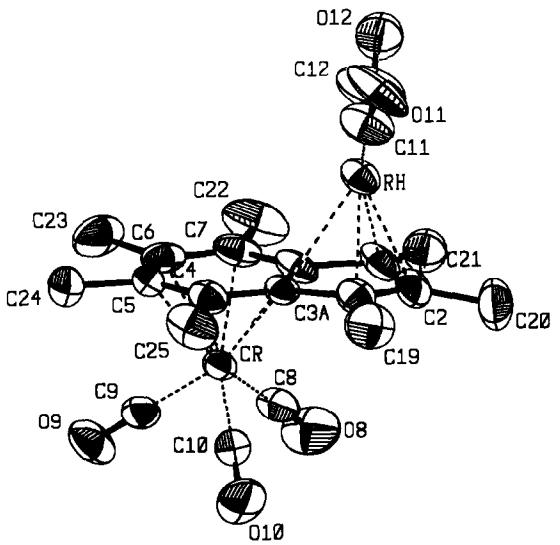

Fig. 1. A perspective view of the molecule of $Cr(CO)_3$-1,2,3,4,5,6,7-heptamethylindenyl-$Rh(CO)_2$ (**A**).

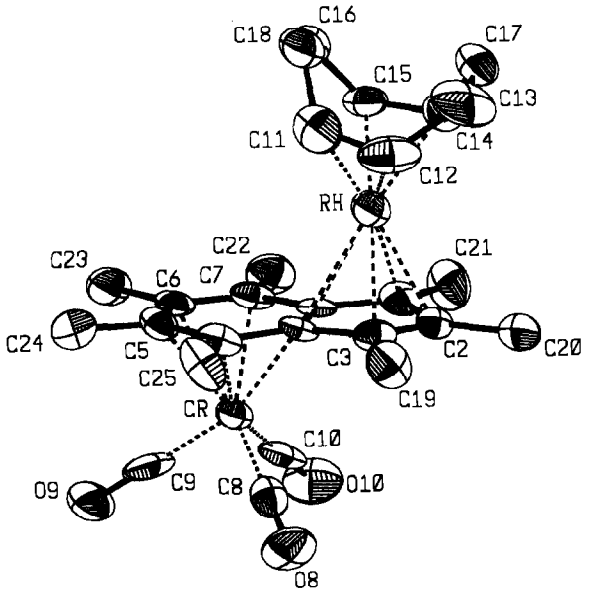

Fig. 2. A perspective view of the molecule of $Cr(CO)_3$-1,2,3,4,5,6,7-heptamethylindenyl-Rh(COD) (**B**).

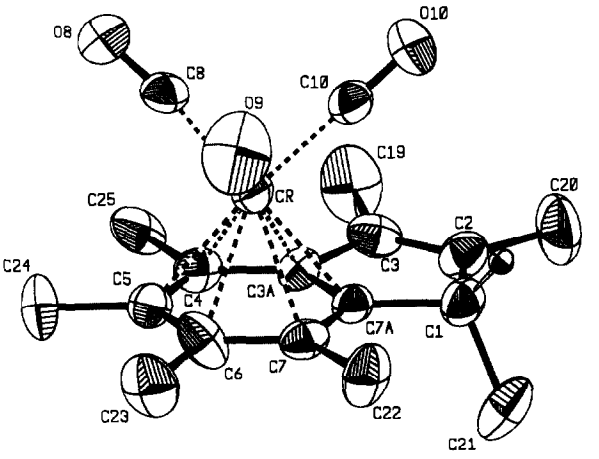

Fig. 3. A perspective view of the molecule of 1-*exo*-CH_3-[$Cr(CO)_3$-1,2,3,4,5,6,7-heptamethylindene] (**C**).

The molecule of **A** displays a pseudo-symmetry C_s with a mirror plane normal to the indenyl ligand through the metal atoms; the group $Rh(CO)_2$ is almost orthogonal to this plane and to the plane defined by C(1)–C(2)–C(3), and this reveals an almost undistorted coordination about Rh. In **B** as well as in the quoted non-methylated homologue [8] the COD ligand assumes the more stable conformation as it results from torsion angles of *ca.* 28–30° about the C(16)–C(18) and C(12)–C(13) bonds, thus relieving the constrained eclipsed conformations found for the corresponding non methylated "*cis*" isomer [20], where COD is almost in its highest C_{2v} symmetry.

2.2. Kinetic measurements

The cyclotrimerization reactions of methyl propiolate (mp) and dimethylacetylenedicarboxylate (dma) were carried out in cyclohexane as solvent by adding a catalytic amount ([alkyne]/[catalyst] 1000/1) of the appropriate Rh catalyst, and they were monitored by *glc*. The time variation of the mp concentration at 50°C by using free and $Cr(CO)_3$-complexed Ind*-Rh(COD) or Ind*-$Rh(CO)_2$ is shown in Fig. 4 and the corresponding kinetic parameters are reported in the upper part of Table 2. For the mono-metallic derivatives, the trimerization reaction stops after 3 h at *ca.* 20% and 40% conversion with Ind*-Rh(COD) and Ind*-$Rh(CO)_2$, respectively, probably because of poisoning of the catalyst. For these complexes, no kinetic data are reported in Table 2.

On the other hand, the catalytic efficiency of the bimetallic substrates is much higher. In fact, the use of

TABLE 2. Catalytic activity of some Ind*-RhL_2 complexes, free and complexed with $Cr(CO)_3$. Solvent, cyclohexane

Methyl propiolate (mp) [a]						
Catalyst	T, °C, ±0.1°C	$10^4 k_{obs.}$ [b]	k_2 [c]	% conversion (t 1 h)	t.o.n. [d] (t 1 h)	product ratio [e]
Ind*–Rh(COD)	50.0	[f]		[f]		
Ind*–$Rh(CO)_2$	50.0	[f]		[f]		
$Cr(CO)_3$–Ind*–Rh(COD)	50.0	5.9	1.1	83	276	52/48
$Cr(CO)_3$–Ind*–$Rh(CO)_2$	50.0	3.0	0.58	68	227	52/48
$Cr(CO)_3$–Ind–Rh(COD)	50.0	12.1	2.3	70	232	70/30
Dimethylacetylenedicarboxylate (dma) [g]						
Catalyst	T, °C, ±0.1°C	$10^3 k_{obs.}$ [b]	k_2	% conversion (t 900 s)	t.o.n. (t 900 s)	$\Delta H^{\ddagger}$ [h], KJ/mol	$\Delta S^{\ddagger}$ [h], J/mol deg
$Cr(CO)_3$–Ind*–Rh(COD)	25.0	0.77	2.0	35.9	485		
$Cr(CO)_3$–Ind*–Rh(COD)	34.0	1.6	4.2	45.7	619		
$Cr(CO)_3$–Ind*–Rh(COD)	42.0	2.8	7.4	87.5	1184		
$Cr(CO)_3$–Ind*–Rh(COD)	50.0	6.0	15.8	99.1	1339	62.5 ± 2.8	−29.8 ± 9.0

[a] $[mp]_0 = 0.526$ mol dm^{-3}; $[cat] = (5.27 \pm 0.01) \times 10^{-4}$ mol dm^{-3}. [b] Initial rates (see text). [c] $k_2 = k_{obs.}/[cat]$; [d] t.o.n. = [trimer][cat]$^{-1}$ h^{-1}; [e] [1,2,4-trimethylbenzene]/[1,3,5-trimethylbenzene] after 24 h; [f] See text; [g] $[dma]_0 = 0.387$ mol dm^{-3}; [h] From Eyring plot.

$Cr(CO)_3$-Ind*-Rh(COD) leads to quantitative conversion of mp to trimers, and the reaction follows the pseudo-first order kinetic law $v = k_{obs.}$[monomer], where $k_{obs.} = k_2$[catalyst]. Under the same conditions, by using $Cr(CO)_3$-Ind*-$Rh(CO)_2$ as catalyst, the above kinetic law is cleanly obeyed up to 70% reaction (*t ca.* 1 h), and in spite of a successive marked decrease of the reaction rate, the monomer conversion was almost complete after 20 h. The good persistence of $Cr(CO)_3$-Ind*-$Rh(CO)_2$ is noteworthy because in the presence of the bimetallic non-methylated $Cr(CO)_3$-Ind-$Rh(CO)_2$, even if the initial rate in the same experimental conditions is comparable, the catalyst is rather unstable in solution since the decrease of the reaction rate occurs after 30 min (45% conversion) [21].

The effect of the permethylation on $Cr(CO)_3$-Ind-Rh(COD) is depicted in Figure 5. It appears that after 2 h the monomer conversion is almost quantitative for the Ind* catalyst, and *ca.* 80% for the non-methylated analogue. Conversely, the initial rate constant is *ca.* one half (see k_2 values in Table 2), and the catalyst was shown by ^{1}H NMR still to be present at the end of the reaction. Both electronic and steric effects of the seven methyl groups can justify the decrease in rate and the higher stability of the Ind* complex.

We also investigated the catalysis reaction at different temperatures using $Cr(CO)_3$-Ind*-Rh(COD), *i.e.*, the more reliable catalyst. Instead of mp dma was used since it is satisfactorily reactive even at lower temperatures. The results obtained in the temperature range 25–50°C are reported in the lower part of Table 2. The enthalpy of activation value (62.5 KJ mol^{-1}) is close to that reported for an associative substitution reaction of CO with phosphines [2c, 5] or olefins (COD, norborna-

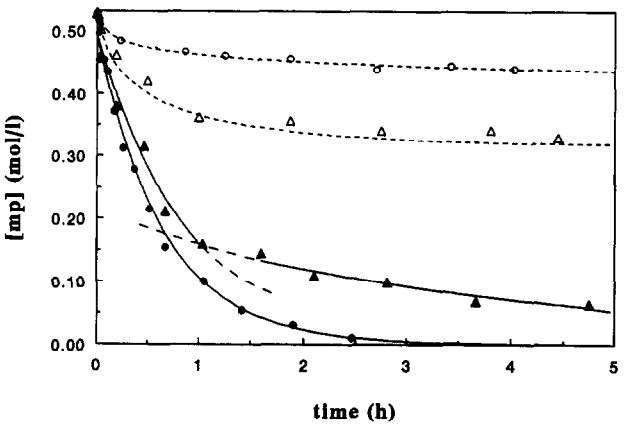

Fig. 4. Monomer disappearance in the methyl propriolate cyclotrimerization reaction catalyzed by Ind*-Rh(COD), ○, Ind*-$Rh(CO)_2$, △, $Cr(CO)_3$-Ind*-Rh(COD), ●, and $Cr(CO)_3$-Ind*-$Rh(CO)_2$, ▲. [Monomer]$_0$, 0.526 mol dm^{-3} in cyclohexane; [monomer]/[cat.] = 1000; T 50.0 ± 0.1°C.

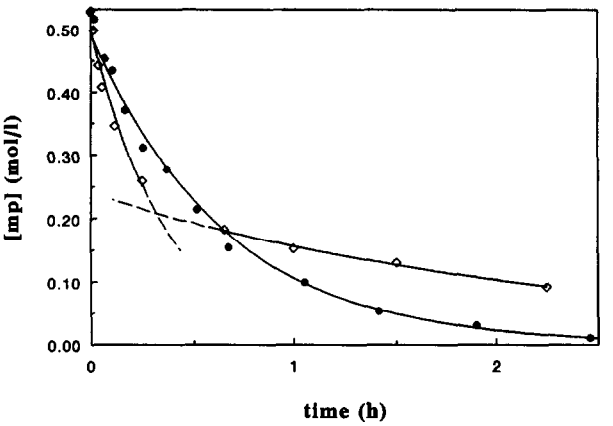

Fig. 5. Monomer disappearance in the methyl propriolate cyclotrimerization reaction catalyzed by $Cr(CO)_3$-Ind*-Rh(COD), ●, and $Cr(CO)_3$-Ind*-Rh(COD), ◇. Experimental conditions as in Fig. 4.

diene [9]) in indenyl complexes. Conversely, the entropy of activation value (−29.8 J mol^{-1} deg^{-1}) is significantly less negative than the values usually found in a simple S_N2 process (*ca.* −80 to −100 J mol^{-1} deg^{-1}).

It has generally been proposed [3c] that the first step in the cyclotrimerization of alkynes in the presence of cyclopentadienyl- or indenyl-RhL_2 catalysts is the substitution of the L ligands by two incoming alkyne molecules. Then, the Ind-Rh(alkyne)$_2$ species, which seems to be the truly active catalyst, isomerizes by a double oxidative addition to give a rhodia(III)-cyclopentadiene intermediate. Subsequently, additional alkyne molecules will displace the butadiene-like subunit yielding the trimer and restoring indenyl-Rh(alkyne)$_2$. However, it is controversial whether both L's are substituted by the alkyne. An alternative mechanism was proposed [22] in which one of the original L ligands is still bonded to rhodium which changes its coordination mode from η^5 to η^3. The higher efficiency exhibited by the indenyl species with respect to the cyclopentadienyl species supports this hypothesis, and the presence of three ancillary ligands π-bonded to rhodium in the course of the catalytic pathway is further supported.

The results of the present work seem to support the second hypothesis. In fact, with complex **B**, the persisting of one (or even both) coordinative bond of COD with rhodium in the trimerization mechanism is supported by the facts that (i) in the course of the reaction the catalyst containing the bidentate COD ligand appears more stable than that containing the monodentate CO, and (ii) the catalyst **B** has been recovered at the end of the reaction, while **A** has not. Moreover, it has been widely demonstrated that the coordination of a *trans*-$Cr(CO)_3$ unit to the indenyl-RhL_2 species in-

duces strong changes of the electronic distribution and, hence, of the coordination mode of rhodium towards the five-membered ring [11]. In particular, the more pronounced η^3 hapticity of the Rh–Cp ring bond upon $Cr(CO)_3$ coordination can be inferred also from the increasing (*ca.* 9 KJ mol^{-1}) of the $\Delta G^{\ddagger}$ value for the rotation around the Rh–indenyl bond.

3. Conclusions

The aim of this work was to improve the efficiency of indenyl-RhL_2 catalysts in trimerization reactions of alkynes.

The reported results indicate that a huge improvement is obtained by using the bimetallic *trans*-(Cr, Rh) indenyl species. An additional benefit was achieved with the bidentate COD as an ancillary ligand to rhodium, since the catalyst becomes more stable and the catalysis rate is higher than that observed for the dicarbonylated species. Finally, the permethylation of the indenyl frame further increases the stability of the catalyst with a moderate reduction of the reaction rate. Thus, the $Cr(CO)_3$-Ind*-Rh(COD) molecule appears the most appropriate one for a detailed study of the mechanism of the alkyne cyclotrimerization.

4. Experimental details

The ^1H and ^{13}C spectra were obtained on a Bruker AM400 spectrometer operating in the FT mode at 400.133 MHz on the proton and 100.614 MHz on the carbon nuclei. $CDCl_3$ and CD_2Cl_2 were used as solvents. The chemical shift values are given with reference to the Me_4Si signal taken as internal standard. The assignment of the ^{13}C lines was based on selective proton decoupling experiments and partially relaxed spectra techniques. For ^1H-{^1H} NOE measurements the usual procedure for gated experiments was modified [22], and the selected multiplet was saturated by a 10 s cyclic perturbation of all lines with a 42 dB attenuation of a nominal 0.2 W decoupling power. The percentage enhancements were obtained from the multiplier of the reference spectrum which brings the multiplet to exact matching of the perturbed spectrum; errors are *ca.* 0.3%.

The IR spectra were recorded as THF solutions (optical length 0.2 mm, CaF_2 windows) on a Perkin Elmer 580B spectrophotometer equipped with a Perkin Elmer 3600 data acquisition system. The 70 eV electron impact mass spectra were recorded on a VG MicroMass-16 spectrometer.

Melting points are uncorrected. All the new complexes gave satisfactory elemental analysis (C, ±0.1; H, ±0.05%). Commercial grade COD was twice distilled and deoxygenated before use. The syntheses and manipulations of all complexes were carried out under a dry, oxygen-free argon atmosphere.

4.1. Syntheses

4.1.1. 1,2,3,4,5,6,7-heptamethylindene

The physical characteristics agree with those reported [11b]. ^1H NMR ($CDCl_3$) 3.155 (d, ^3J 7.3 Hz, 1-H), 2.486 (s, 3H, 7-CH_3), 2.300 (s, 3H, 4-CH_3), 2.225 (s, 3H, 5-CH_3), 2.220 (s, 3H, 6-CH_3), 2.211 (m, 3H, 3-CH_3), 1.927 (m, 3H, 2-CH_3), and 1.211 (d, ^3J 7.3 Hz, 3H, 1-CH_3); ^{13}C NMR: δ 144.86 (C_2), 140.83 (C_{7a}), 142.89 (C_{3a}), 133.75, 131.90, 130.75, 128.35 (C_4-C_7), 126.37 (C_3), 46.26 (C_1), 16.57 (4-CH_3), 16.29 (6-CH_3), 16.10 (5-CH_3), 15.98 (1-CH_3), 15.85 (7-CH_3), 15.22 (3-CH_3), and 12.23 (2-CH_3).

4.1.2. (1-exo-CH_3)- and (1-endo-CH_3)$Cr(CO)_3$-1,2,3,-4,5,6,7-heptamethylindene

The ligand was reacted with $(NH_3)_3Cr(CO)_3$ in refluxing dioxane as previously reported [11]. Conversion was 60%. TLC analysis indicated the presence of two isomers (in the ratio 85/15, as measured by NMR signal integration) which were separated by medium pressure liquid chromatography (petroleum ether as eluent) and crystallized from pentane.

4.1.3. (1-endo-CH_3)-$Cr(CO)_3$-1,2,3,4,5,6,7-heptamethylindene

Yield, 15%. M.p. 130–134°C; *m/z* 350 (M^+). IR: ν_{max} (THF): 1943vs and 1862vs cm^{-1} (C≡O). ^1H NMR: δ 3.210 (q, ^3J 7.2 Hz, 1H, 1-H), 2.401 (s, 3H, 4-CH_3), 2.341 (s, 3H, 7-CH_3), 2.289 (s, 3H, 6-CH_3), 2.151 (s, 3H, 5-CH_3), 2.144 (m, 3H, 2-CH_3), 1.909 (m, 3H, 2-CH_3), and 1.394 (d, ^3J 7.2 Hz, 3H, 1-CH_3); ^{13}C NMR: δ 236.00 (C≡O), 147.98 (C_2), 129.96 (C_3), 120.50 (C_{7a}), 119.05 (C_{3a}), 117.57, 116.49, 116.07, 110.17 (C_7-C_4), 45.88 (C_1), 19.91 (4-CH_3), 16.51 (1-CH_3), 16.38, 16.06, 16.01 (5-CH_3, 6-CH_3, 7-CH_3), 14.69 (3-CH_3), and 12.76 (2-CH_3).

4.1.4. (1-exo-CH_3)-$Cr(CO)_3$-1,2,3,4,5,6,7-heptamethylindene

Yield, 85%. M.p. 115–119°C; *m/z* 350 (M^+). IR: ν_{max} (THF): 1945vs and 1866vs cm^{-1} (C≡O). ^1H NMR: δ 3.314 (q, ^3J 7.2 Hz, 1H, 1-H), 2.471 (s, 3H, 4-CH_3), 2.361 (s, 3H, 7-CH_3), 2.228 (s, 3H, 6-CH_3), 2.189 (s, 3H, 5-CH_3), 2.128 (m, 3H, 3-CH_3), 1.903 (m, 3H, 2-CH_3), and 1.234 (d, ^3J 7.2 Hz, 3H, 1-CH_3); ^{13}C NMR: δ 235.71 (C≡O), 146.35 (C_2), 130.05 (C_3), 118.36 (C_{3a}), 113.87 (C_{7a}), 107.26, 105.32, 103.34, 102.30 (C_7-C_4), 46.69 (C_1), 17.39 (4-CH_3), 16.39 (6-CH_3), 16.35 (1-CH_3), 16.19 (5-CH_3), 15.84 (7-CH_3), 14.54 (3-CH_3),

and 12.51 (2-CH_3). The *exo* position of the 1-CH_3 group was confirmed by the crystal structure of the complex (see below).

4.1.5. 1,2,3,4,5,6,7-Heptamethylindenyl-Rh(COD)

Ind*-Rh(COD) was obtained by reacting a 0.1 M THF solution of 1,2,3,4,5,6,7-heptamethylindene with a slight excess of LiBu in the presence of TMEDA at room temperature. The orange solution was added to an equivalent quantity of [Rh(μ-Cl)(COD)]$_2$ dissolved in THF and the solvent evaporated obtaining an orange residue which was extracted with pentane. Crystallization from hexane gave the product in 56% yield. M.p. 164–168°C (decomp.); *m/z* 424 (M^+); ^{1}H NMR: (CD_2Cl_2) δ 3.391 (m, 4H, =C–H COD protons), 2.391 (s, 6H, 4,7-CH_3), 2.200 (s, 6H, 5,6-CH_3), 2.168 (d, 3H, $J(^{103}Rh–H_2)$ 1.5 Hz, 2-CH_3), 2.052 (s, 6H, 1.3-CH_3), and 1.9–1.7 (m, 8H, CH_2 COD protons); ^{13}C NMR: δ 128.87 (5,6-CH_3), 123.73 (4,7-CH_3), 109.67 ($^1J(^{103}Rh–^{13}C)$ 2.4 Hz, C_{3a},C_{3a}), 107.61 ($^1J(^{103}Rh–^{13}C)$ 5.6 Hz, C_2), 85.91 ($^1J(^{103}Rh–^{13}C)$ 4.2 Hz, $C_{1,3}$), 17.00 (4,7-CH_3), 16.68 (5,6-CH_3), 12.91 (1,3-CH_3), and 11.43 ($^1J(^{103}Rh–^{13}C)$ *ca.* 1 Hz, 2-CH_3).

4.1.6. 1,2,3,4,5,6,7-Heptamethylindenyl-Rh(CO)$_2$

Ind*-Rh(CO)$_2$ was obtained by bubbling CO through an Ind*-Rh(COD) solution in CH_2Cl_2 until the reagent had disappeared. Evaporation of the solvent gave the product in quantitive yield. M.p. 127–131°C (decomp.); *m/z* 372 (M^+); IR (CH_2Cl_2): ν_{max} 2024s and 1963 cm^{-1} (C≡O); ^{1}H NMR (CD_2Cl_2): δ 2.481 (s, 6H, 5,6-CH_3), 2.479 (s, 6H, 1.3-CH_3), 2.197 (s, 6H 4,7-CH_3), and 2.180 (d, 3H, $J(^{103}Rh–H_2)$ 2.2 Hz, 2-CH_3); ^{13}C NMR: δ 192.84 ($^1J(^{103}Rh–^{13}C)$ 86.4 Hz, Rh–*C*≡O), 132.61 (5,6-CH_3), 123.68 (4,7-CH_3), 114.92 ($^1J(^{103}Rh–^{13}C)$ 6.8 Hz, C_2), 113.95 ($^1J(^{103}Rh–^{13}C)$ 2.3 Hz, C_{3a},C_{7a}), 90.00 ($^1J(^{103}Rh–^{13}C)$ 3.8 Hz, $C_{1,3}$), 16.83 (5,6-CH_3), 16.58 (4,7-CH_3), 15.16 (1,3-CH_3), and 12.41 ($^1J(^{103}Rh–^{13}C)$ 2.3 Hz, 2-CH_3).

4.1.7. Cr(CO)$_3$-1,2,3,4,5,6,7-heptamethylindenyl-Rh-(COD)

To a yellow THF solution of (1-exo-CH_3)-Cr(CO)$_3$-1,2,3,4,5,6,7-heptamethylindene cooled at −30°C a slight excess of BuLi in hexane in the presence of TMEDA was added and the colour changed instanta-

TABLE 3. Summary of the crystal data and intensity data collection for **A**, **B** and **C**

	A	**B**	**C**
Formula	$C_{21}H_{21}CrO_5Rh$	$C_{27}H_{33}CrO_3Rh$	$C_{19}H_{30}CrO_3$
M	508.29	560.44	358.43
Crystal dim/mm	0.20 × 0.20 × 0.30	0.30 × 0.30 × 0.25	0.20 × 0.15 × 0.25
T/K	298	298	298
Radiation	graphite monochromated Mo Kα (λ = 0.7107)		
Space group	$P\bar{1}$	*Pbca*	*P*1
a/Å	9.120(5)	21.866(9)	9.093(5)
b/Å	9.366(5)	16.080(7)	9.812(5)
c/Å	13.648(6)	13.985(6)	10.847(5)
α/°	95.3(1)	90	66.2(1)
β/°	103.2(1)	90	79.8(2)
γ/°	111.5(1)	90	83.0(2)
V/Å^3	1035.87	4917.20	870.11
Z	2	8	2
D_c/g cm^{-3}	1.63	1.51	1.37
F(000)	512	2304	384
μ/cm^{-1}	14.14	11.89	8.25
Scan speed/deg mm^{-1}	2.0 in the 2ϑ scan mode		
Scan width/deg	1.2	1.2	1.2
Take off angle/deg	3	3	3
2ϑ range	$3.0 < 2\vartheta < 45$		
Total reflections	3230	1647	2627
Reflections used for refinement [a]	2897	1277	2439
Solution methods	Patterson	Patterson	Patterson
Hydrogen atoms detected	21	14	19
Refined parameters	337	289	208
R [b] (on F_o)	0.026	0.032	0.055
R_w [c]	0.029	0.032	0.063
Goodness of fit [d]	0.907	0.499	1.337
Highest map residuals, e/Å^3	0.88	0.048	0.245

[a] $F_o^2 > 2\sigma(F_o^2)$; [b] $R = \Sigma||F_o| - |F_c||/\Sigma|F_o|$; [c] $R_w = [\Sigma w(||F_o| - |F_c||)^2/\Sigma wF_0^2]^{1/2}$; [d] G.O.F. = $[\Sigma w(||F_o| - |F_c||)^2/(NO - NV)^2]^{1/2}$.

TABLE 4. Fractional coordinates with equivalent isotropic thermal parameters/Å^2 for (1-exo-CH_3)-Cr(CO)$_3$-1,2,3,4,5,6,7-heptamethylindene, *trans*-Cr(CO)$_3$-1,2,3,4,5,6,7-heptamethylindenyl-Rh(COD), and *trans*-Cr(CO)$_3$-1,2,3,4,5,6,7-heptamethylindenyl-Rh(CO)$_2$. U_{eq} is defined as one third of the trace of the orthogonalized U_{ij} tensor

Atom	x	y	z	U_{eq}
(1-exo-CH$_3$)-Cr(CO)$_3$-1,2,3,4,5,6,7-heptamethylindene				
Cr	0.3203(1)	0.1876(1)	0.2487(1)	0.0391(4)
O(8)	0.5898(7)	0.3024(7)	0.2881(6)	0.078(3)
O(9)	0.1432(8)	0.4619(7)	0.2496(8)	0.098(4)
O(10)	0.2384(6)	0.0323(7)	0.5481(5)	0.074(3)
C(8)	0.4851(8)	0.2588(8)	0.2748(7)	0.050(3)
C(9)	0.2120(9)	0.3565(9)	0.2517(9)	0.061(4)
C(10)	0.2707(8)	0.0915(8)	0.4333(8)	0.052(3)
C(1)	0.1201(7)	−0.1166(8)	0.3210(7)	0.045(3)
C(2)	0.2394(8)	−0.2292(8)	0.3887(7)	0.047(3)
C(3)	0.3774(8)	−0.1828(8)	0.3353(7)	0.046(3)
C(3a)	0.3653(4)	−0.0291(4)	0.2237(4)	0.037(3)
C(4)	0.4709(4)	0.0699(4)	0.1340(4)	0.041(3)
C(5)	0.4241(4)	0.2089(4)	0.0421(4)	0.040(3)
C(6)	0.2717(4)	0.2488(4)	0.0399(4)	0.042(2)
C(7)	0.1661(4)	0.1497(4)	0.1295(4)	0.043(3)
C(7a)	0.2129(4)	0.0108(4)	0.2215(4)	0.037(2)
C(19)	0.5215(8)	−0.2686(8)	0.3799(9)	0.062(4)
C(20)	0.195(1)	−0.373(1)	0.5047(9)	0.073(4)
C(21)	0.0298(8)	−0.1791(9)	0.2503(9)	0.063(4)
C(22)	−0.0037(7)	0.1955(8)	0.1327(8)	0.056(4)
C(23)	0.2183(9)	0.3980(9)	−0.0670(8)	0.066(4)
C(24)	0.5409(8)	0.3170(9)	−0.0567(8)	0.057(3)
C(25)	0.6413(7)	0.0262(9)	0.1354(7)	0.053(3)
trans-Cr(CO)$_3$-1,2,3,4,5,6,7-heptamethylindenyl-Rh(COD)				
Rh	0.15001(4)	0.51846(5)	0.62719(7)	0.0443(3)
Cr	0.09904(7)	0.3558(1)	0.8724(1)	0.0361(6)
O(8)	0.1348(4)	0.4517(5)	1.0454(6)	0.073(4)
O(9)	0.0168(4)	0.2484(7)	0.9866(6)	0.104(5)
O(10)	0.1983(4)	0.2331(5)	0.9066(6)	0.075(4)
C(1)	0.2044(5)	0.4284(7)	0.7085(8)	0.044(5)
C(2)	0.2164(5)	0.5064(7)	0.7489(7)	0.033(5)
C(3)	0.1618(5)	0.5395(6)	0.7862(7)	0.039(5)
C(3a)	0.1147(5)	0.4736(8)	0.7802(7)	0.033(4)
C(4)	0.0530(5)	0.4682(6)	0.8110(7)	0.038(4)
C(5)	0.0188(5)	0.3982(7)	0.7887(8)	0.042(5)
C(6)	0.0455(6)	0.3281(7)	0.7431(7)	0.041(5)
C(7)	0.1072(6)	0.3303(7)	0.7163(7)	0.040(5)
C(7a)	0.1435(6)	0.4038(7)	0.7330(7)	0.032(4)
C(8)	0.1218(5)	0.4141(7)	0.9788(9)	0.045(5)
C(9)	0.0505(6)	0.2904(8)	0.9412(8)	0.060(6)
C(10)	0.1601(6)	0.2807(7)	0.8932(7)	0.052(5)
C(11)	0.0807(6)	0.5949(8)	0.5619(9)	0.068(6)
C(12)	0.1301(7)	0.6432(8)	0.5871(9)	0.075(6)
C(13)	0.1776(7)	0.6720(8)	0.5149(9)	0.096(7)
C(14)	0.1977(5)	0.5193(8)	0.4946(7)	0.055(5)
C(15)	0.1500(5)	0.4621(7)	0.4872(7)	0.051(5)
C(16)	0.0910(5)	0.4825(9)	0.4359(8)	0.067(6)
C(17)	0.2003(6)	0.6042(8)	0.4487(8)	0.072(6)
C(18)	0.0657(5)	0.567(1)	0.4609(9)	0.078(6)
C(19)	0.1570(6)	0.6195(7)	0.8377(8)	0.064(5)
C(20)	0.2753(5)	0.5527(7)	0.7514(8)	0.061(5)
C(21)	0.2547(5)	0.3747(8)	0.6679(8)	0.064(6)
C(22)	0.1373(5)	0.2557(7)	0.6685(8)	0.060(5)
C(23)	0.0078(6)	0.2537(7)	0.7205(9)	0.067(6)
C(24)	−0.0493(5)	0.3957(8)	0.8149(8)	0.065(5)
C(25)	0.0248(5)	0.5405(6)	0.862(1)	0.069(5)

TABLE 4 (continued)

Atom	x	y	z	U_{eq}
[Cr(CO)$_3$-1,2,3,4,5,6,7-heptamethylindenyl]Rh(CO)$_2$				
Rh	0.08201(3)	0.56140(2)	0.83240(2)	0.0439(1)
Cr	0.32882(5)	0.92567(5)	0.66632(3)	0.0364(2)
O(8)	0.3417(4)	1.2217(3)	0.7771(3)	0.090(1)
O(9)	0.3768(3)	1.1005(3)	0.4971(2)	0.072(1)
O(10)	0.6941(3)	1.0395(4)	0.7414(2)	0.079(1)
O(11)	0.0761(5)	0.2505(4)	0.8676(4)	0.135(3)
O(12)	−0.2767(4)	0.4586(5)	0.8122(4)	0.147(3)
C(1)	0.1565(5)	0.8171(3)	0.8584(3)	0.054(1)
C(2)	0.2836(5)	0.7876(3)	0.9206(2)	0.068(1)
C(3)	0.3477(4)	0.7112(3)	0.8580(2)	0.046(1)
C(3a)	0.2807(3)	0.7212(3)	0.7510(2)	0.036(1)
C(4)	0.3133(3)	0.6794(3)	0.6575(2)	0.042(1)
C(5)	0.2140(4)	0.6899(3)	0.5646(2)	0.048(1)
C(6)	0.0909(4)	0.7498(3)	0.5657(2)	0.052(1)
C(7)	0.0639(4)	0.7998(4)	0.6573(3)	0.051(1)
C(7a)	0.1588(3)	0.7839(3)	0.7510(2)	0.042(1)
C(8)	0.3376(4)	1.1063(4)	0.7368(3)	0.053(1)
C(9)	0.3587(3)	1.0310(4)	0.5619(2)	0.048(1)
C(10)	0.5529(4)	0.9956(4)	0.7130(2)	0.047(1)
C(11)	0.0795(5)	0.3663(4)	0.8479(3)	0.069(2)
C(12)	−0.1418(5)	0.4938(5)	0.8188(4)	0.080(2)
C(19)	0.4889(5)	0.6649(5)	0.8988(3)	0.076(2)
C(20)	0.3435(7)	0.8301(5)	1.0369(3)	0.094(3)
C(21)	0.0684(7)	0.9057(5)	0.9016(4)	0.096(3)
C(22)	−0.0686(5)	0.8598(5)	0.6613(4)	0.087(2)
C(23)	−0.0110(5)	0.7590(5)	0.4622(3)	0.087(2)
C(24)	0.2374(5)	0.6379(5)	0.4635(3)	0.078(2)
C(25)	0.4438(4)	0.6176(4)	0.6575(3)	0.065(2)

neously to orange. The solution was quickly added to one equivalent of [Rh(μ-Cl)(COD)]$_2$ dissolved in THF and maintained at −30°C and an immediate change of colour to deep red was observed. After few minutes the solvents were evaporated obtaining a brown residue which was extracted with CH_2Cl_2 and then purified by flash chromatography on silica. Yield, 30%; *m/z* 560 (M^+); IR (THF): ν_{max} 1937vs, 1861vs and 1851vs cm^{-1} (C≡O); ^{1}H NMR (CD_2Cl_2): δ 3.689 (m, 4H, =C–H COD protons), 2.599 (s, 6H, 4,7-CH_3), 2.197 (s, 6H, 5,6-CH_3), 2.105 (d, 3H, $^1J(^{103}Rh–H)$ 1.8 Hz, 2-CH_3), 2.043 (s, 6H, 1,3-CH_3), and 1.95 (m, 8H, CH_2 COD protons); ^{13}C NMR: δ 236.65 (Cr–*C*≡O), 118.77 (d, $^1J(^{103}Rh–^{13}C)$ 5.6 Hz, C_2), 104.63 ($C_{5,6}$), 98.89 ($C_{4,7}$), 85.44 (d, $^1J(^{103}Rh–^{13}C)$ 4.2 Hz, $C_{1,3}$), 84.38 (d, $^1J(^{103}Rh–^{13}C)$ 2.4 Hz, $C_{3a,7a}$), 73.47 (d, $^1J(^{103}Rh–^{13}C)$ 13.3 Hz, =*C*–H COD carbons), 31.77 (CH_2 COD carbons), 17.59 (5,6-CH_3), 16.81 (4,7-CH_3), 12.63 (1,3-CH_3), and 12.00 (d, $^1J(^{103}Rh–^{13}C)$ 1.8 Hz, 2-CH_3).

4.1.8. Cr(CO)$_3$-1,2,3,4,5,6,7-heptamethylindenyl-Rh-(CO)$_2$.

This complex was obtained by bubbling CO into a solution of Cr(CO)$_3$-1,2,3,4,5,6,7-heptamethylindenyl-

Rh(COD) in CH_2Cl_2. Evaporation of the solvent gave quantitatively the red product. M.p. 127–131°C (decomp.); m/z 508 (M^+); IR (CH_2Cl_2): ν_{max} 2043s, 1985s, 1941vs, and 1862vs cm^{-1} (C≡O); ^1H NMR (CD_2Cl_2): δ 2.603 (s, 6H, 5,6-CH_3), 2.449 (s, 6H, 1,3-CH_3), 2.147 (s, 6H, 4,7-CH_3), and 2.129 (d, $J(^{103}Rh-H)$ 2.6 Hz, 3H, 2-CH_3); ^{13}C NMR: δ 235.53 (Cr–C≡O), 189.99 (d, $^1J(^{103}Rh-^{13}C)$ 87.1 Hz, Rh–C≡O), 126.66 (d, $^1J(^{103}Rh-^{13}C)$ 7.0 Hz, C_2), 106.15 ($C_{5,6}$), 98.42 ($C_{4,7}$), 88.74 (d, $^1J(^{103}Rh-^{13}C)$ 2.0 Hz, $C_{3a,7a}$), 88.58 (d, $^1J(^{103}Rh-^{13}C)$ 3.8 Hz, $C_{1,3}$), 18.91 (4,7-CH_3), 18.86 (5,6-CH_3), 15.02 (1,3-CH_3), and 13.36 (d, $^1J(^{103}Rh-^{13}C)$ 2.6 Hz, 2-CH_3).

4.2. Collection of X-ray diffraction data

X-ray-quality crystals of (1-exo-CH_3)-$Cr(CO)_3$-1,2,3,4,5,6,7-heptamethylindene (**C**), $Cr(CO)_3$-1,2,3,4,5,6,7-heptamethylindenyl-Rh(COD) (**B**) and $Cr(CO)_3$-1,2,3,4,5,6,7-heptamethylindenyl-$Rh(CO)_2$ (**A**) were grown from saturated solutions in an 1:1 mixture of methylene chloride/pentane (**A**), and pentane (**B** and **C**). Single crystals were mounted on a Philips PW-100 computer-controlled four-circle diffractometer with graphite monochromator. Standard centring and autoindexing procedures indicated a primitive orthorhombic lattice, space group *Pbca* for **B**, and triclinic lattices for **A** and **C**, for which the space group $P\bar{1}$ was initially assigned and later confirmed by well-behaved refinement process. The orientation matrix and accurate unit cell dimensions were determined from angular settings of 25 high-angle reflections. The intensities were corrected for Lorentz and polarization effects and for absorption by empirical methods (Ψ-scan). Crystallographic data are consolidated in Table 3. In all cases the structures were solved from Patterson syntheses and completed from difference maps. All non-hydrogen atoms were refined with anisotropic thermal parameters. All the hydrogen atoms for **A** and a large part for **B** and **C** (see Table 3) were located from difference Fourier syntheses, the remaining were geometrically determined. Blocked-cascade least-square refinements were used. They converged to the conventional R indices reported in Table 3. A unitary weighting scheme was used. Scattering factors for the atoms were taken from Cromer and Waber [23]; the scattering factors for Cr and Rh were corrected for the real and the imaginary parts of anomalous dispersion using Cromer's values [24]. All computations were carried out on a Cyber 76 computer using the SHELX-76 program [25]. The final positional parameters of the non-hydrogen atoms are listed in Table 4.

The anisotropic thermal parameters of the non-hydrogen atoms, the positional parameters of the hydrogen atoms, full lists of bond lengths and angles, and lists of calculated and observed structure factors are available as supplementary material.

4.3. Catalysis experiments

To a 0.56 M solution of methyl propiolate (mp) in cyclohexane thermostatted at 50.0 ± 0.1°C the catalytic amount of the indenyl derivative was added ([methyl propriolate]/[catalyst] = 1000/1). The disappearance of the monomer was monitored by GLC ($T_{inj.} = T_{det.} =$ 180°C; T_c 120°C; FID detector; flow, 30 ml/min N_2; column, 1/8″ i.d., 2 m length; stationary phase, SE-30 20% on Chromsorb P); *o*-xylene was used as external standard for integration. In the case of dimethylacetylenedicarboxylate (dma), the initial concentration was 0.387 M. The catalytic runs were performed in the temperature interval 25.0 ± 0.1 to 50.0 ± 0.1°C. In the case of mp, the product ratio 1,2,4-tricarboxymethyl-benzene/ 1,3,5-tricarboxymethyl-benzene was measured by NMR integration of the corresponding ^1H signals (solvent $CDCl_3$).

Acknowledgement

This work was supported in part by the Consiglio Nazionale delle Ricerche (CNR, Roma) through its Progetto Finalizzato Chimica Fine II.

References

1 (a) C. White and R.J. Mawby, *Inorg. Chim. Acta*, *4* (1970) 261; (b) C. White, R.J. Mawby and A.J. Hart-Davis, *Inorg. Chim. Acta*, *4* (1970) 441; (c) D.J. Jones and R.J. Mawby, *Inorg. Chim. Acta*, *6* (1972) 157; (d) N.N. Turaki, J.M. Huggins and L. Labioda, *Inorg. Chem.*, *27* (1988) 424.

2 (a) P. Caddy, M. Green, E. O'Brien, L.E. Smart and P. Woodward, *J. Chem. Soc., Dalton Trans.*, (1980) 962; *Angew. Chem., Int. Ed. Engl.*, *16* (1977) 648; (b) M.E. Rerek and F. Basolo, *J. Am. Chem. Soc.*, *106* (1984) 5908; (c) L.-N. Ji and F. Basolo, *Organometallics*, *3* (1984) 740; (e) A.J. Hart-Davis and R.J. Mawby, *J. Chem. Soc. A*, (1969) 2403; (f) T.B. Marder and I.D. Williams, *J. Chem. Soc., Chem. Commun.*, (1987) 1478; (g) A.K. Kakkar, N.J. Taylor and T.B. Marder, *Organometallics*, *8* (1989) 1765; (h) H. Estiagh-Hosseini and J.F. Nixon, *J. Less-Common Met.*, *61* (1978) 107; (i) D.A. Brown, N.J. Fitzpatrick, W.K. Glass, H.A. Hamed, D. Cunningham and P. McArdle, *J. Organomet. Chem.*, *455* (1993) 157; (j) L. Ambrosi, M. Bassetti, P. Buttiglieri, L. Mannina, D. Monti and G. Bocelli, *J. Organomet. Chem.*, *455* (1993) 167.

3 (a) T.B. Marder, D.C. Roe and D. Milstein, *Organometallics*, *7* (1988) 1451; (b) P. Caddy, M. Gree, L.E. Smart and N. White, *J. Chem. Soc., Chem. Commun.*, (1978) 839; (c) A. Borrini, P. Diversi, G. Ingrosso, A. Lucherini and G. Serra, *J. Mol. Catal.*, *24* (1985) 181; (d) H. Bonneman and W. Brijoux, in R. Ugo (ed.), *Aspects of Homogenoeos Catalysis*, Vol. 5, Dordrecht, 1984, p. 75.

4 T.C. Forschner, A.R. Cutler and R.K. Kullnig, *Organometallics*, *6* (1987) 889; H. Amhed, D.A. Brown, N.J. Fitzpatrick and W.K. Glass, *J. Organomet. Chem.*, *418* (1991) C14.

5 H. Bang, T.J. Lynch and F. Basolo, *Organometallics*, *11* (1992) 40.

6 J.S. Merola, R.T. Kacmarcik and Donna Van Engen, *J. Am. Chem. Soc.*, *108* (1986) 329.

7 S. Bellomo, A. Ceccon, A. Gambaro, S. Santi and A. Venzo, *J. Organomet. Chem.*, *453* (1993) C4.

8 A. Ceccon, A. Gambaro, S. Santi, G. Valle and A. Venzo, *J. Chem. Soc., Chem. Commun.*, (1989) 51.

9 C. Bonifaci, A. Ceccon, A. Gambaro, S. Santi and A. Venzo, *Xth FECHEM Conference on Organometallic Chemistry*, Agia Pelagia, Crete, Greece, September 5–11, 1993, Abstr. p. 96; C. Bonifaci, A. Ceccon, A. Gambaro, S. Santi and A. Venzo, *Inorg. Chim. Acta*, submitted.

10 A. Ceccon, A. Gambaro, S. Santi and A. Venzo, *J. Mol. Catal.*, *69* (1991) L1–L6

11 A. Ceccon, C.J. Elsevier, J.M. Ernsting, A. Gambaro, S. Santi and A. Venzo, *Inorg. Chim. Acta*, *204* (1993) 15.

12 P.G. Gassman, J.W. Mickelson and J.R. Sowa, *J. Am. Chem. Soc.*, *114* (1992) 6942; D.P. Drolet and A.J. Lees, *J. Am. Chem. Soc.*, *114* (1992) 4186; P.M. Maitlis, *Acc. Chem. Res.*, *12* (1980) 121; P.M. Maitlis, *Acc. Chem. Res.*, *11* (1978) 301; S.J. McLain, J. Sancho and R.R. Schrock, *J. Am. Chem. Soc.*, *101* (1979) 5451; J.M. Manriquez, P.J. Fagan and T.J. Marks, *J. Am. Chem. Soc.*, *100* (1978) 3939; D.J. Sykora, M.D. Rausch, R.D. Rogers and J.L. Atwood, *J. Am. Chem. Soc.*, *103* (1981) 1265; D.P. Freyberg, J.L. Robbins, K.N. Raymond and J.C. Smart, *J. Am. Chem. Soc.*, *101* (1979) 892; R.B. King, *Coord. Chem. Rev.*, *20* (1976) 155; G. Jeske, H. Lauke, H. Mauermann, P.N. Swepston, H. Schumann and T.J. Marks, *J. Am. Chem. Soc.*, *107* (1985) 8091; M.E. Rerek and F. Basolo, *J. Am. Chem. Soc.*, *106* (1984) 5908; R. Cramer and L.P. Seiwell, *J. Organomet. Chem.*, *92* (1975) 245.

13 (a) D. O'Hare, V.J. Murphy and N. Kaltsoyannis, *J. Chem. Soc., Dalton Trans.*, (1993) 383; (b) D. O'Hare, J.C. Green, T.B. Marder, S. Collins, G. Stringer, A.K. Kakkar, N. Kaltsoyannis, A. Kuhn, R. Lewis.C. Menhert, P. Scott, M. Kurmoo and S. Pugh, *Organometallics*, *11* (1992) 48.

14 A.K. Kakkar, S.F. Jones, N.J. Taylor, S. Collins and T.B. Marder, *J. Chem. Soc., Chem. Commun.*, (1989) 1454.

15 A.K. Kakkar, N.J. Taylor, T.B. Marder, J.K. Shen, N. Hallinan and F. Basolo, *Inorg. Chim. Acta*, *198–200* (1992) 219.

16 A. Ceccon, A. Gambaro, F. Manoli, P. Ganis, G. Valle, A. Venzo and D. Kuck, *Chem. Ber.*, *126* (1993) 2053; A. Ceccon, A. Gambaro, F. Manoli, A. Venzo, D. Kuck, P. Ganis and G. Valle, *J. Chem. Soc., Perkin Trans. II*, (1992) 1111; A. Ceccon, A. Gambaro, F. Manoli, A. Venzo, D. Kuck, T.E. Bitterwolf, P. Ganis, G. Valle, *J. Chem. Soc., Perkin Trans. II*, (1991) 233.

17 A. Ceccon, A. Gambaro, F. Gottardi, S. Santi and A. Venzo, *J. Organomet. Chem.*, *412* (1991) 85.

18 H. Günther, *NMR Spectroscopy: An Introduction*, John Wiley & Sons, New York, 1980.

19 P. Berno, A. Ceccon, A. Gambaro, A. Venzo, P. Ganis and G. Valle, *J. Chem. Soc., Perkin Trans. II*, (1987) 935.

20 (a) C. Bonifaci, A. Ceccon, A. Gambaro, P. Ganis, S. Santi, G. Valle and A. Venzo, *Xth FECHEM Conference on Organometallic Chemistry*, Agia Pelagia, Crete, Greece, September 5–11, 1993, Abstr.p. 224; (b) C. Bonifaci, A. Ceccon, A. Gambaro, P. Ganis, S. Santi, G. Valle and A. Venzo, manuscript in preparation.

21 C. Bonifaci, A. Ceccon, A. Gambaro, S. Santi and A. Venzo, to be published.

22 K. Abdulla, B.L. Booth and C. Stacey, *J. Organomet. Chem.*, *293* (1985) 103.

23 A. Ceccon, A Gambaro, F. Gottardi, S. Santi, A. Venzo and V. Lucchini, *J. Organomet. Chem.*, *379* (1989) 67.

24 D.T. Cromer, J.T. Waber, *Acta Crystallogr.*, *18* (1965) 184.

25 D.T. Cromer, *Acta Crystallogr.*, *18* (1965) 17.

26 G.M. Sheldrick, SHELX-76, Program for Crystal Structure Determination, Cambridge University, England, 1976.